COVID-19 Prediction Based on DWT and Moment Invariant Features of Radiography Image Using the Artificial Neural Network Classifier

Ditha Nurcahya Avianty[1], I Gede Pasek Suta Wijaya[1*], Fitri Bimantoro[1], Rina Lestari[2], and Triana Dyah Cahyawati[2]

[1]*Department Informatics Engineering, University of Mataram, Indonesia*
[2]*Faculty of Medicine, University of Mataram, Indonesia*
[*]*Corresponding author. Email: gpsutawijaya@unram.ac.id*

ABSTRACT
COVID-19 is an infectious disease caused by a family of coronaviruses, namely severe acute respiratory syndrome coronavirus 2 (SARS-CoV-2). The fastest method to identify the presence of this virus is a rapid antibody or antigen test, but to confirm the positive status of a COVID-19 patient, further examination is recommended. Lung examination using chest radiography images taken through X-rays of COVID-19 patients can be one of the method to confirm the patient's condition before/after the rapid test. In this paper, a model to detect COVID-19 through chest radiography images is proposed by using a combination of Discrete Wavelet Transform (DWT) and Moment Invariant features, and the Artificial Neural Network (ANN) classifiers. In this case, the haar wavelet transform and seven Hu moments were used to extracting the image's features. The main aim of the work is to find the best features and ANN model for predicting chest radiography images as COVID-19 suspect, pneumonia, or normal. The k-fold cross-validation test on the best parameters obtained accuracy up to 86.32%, a precision level of 86.35%, and a recall rate of 86.26%.

Keywords: *COVID-19, Radiographic Image, Artificial Neural Network, Discrete Wavelet Transform, Moment Invariant.*

1. INTRODUCTION

Corona Virus Disease or known as COVID-19 is an infectious diseases caused by *severe acute respiratory syndrome coronavirus* 2 (SARS-CoV-2). The disease was unknown before the outbreak began in Wuhan, China in December 2019 [1]. The spread of COVID-19 occurs very quickly and widely because its spread can occur from human to human contact through direct contact [2]. The recommended method for the COVID-19 detection is nucleic acid amplification with real-time Reverse Transcription Polymerase Chain Reaction (rt-PCR) or repeated swab tests. [3]. This method relies on expensive facilities, trained health workers, and often requires a long time in the testing process, causing delays in disease prevention efforts [4]. Delays in test results and lack of test kits make it difficult for many countries to identify the number of positive cases of COVID-19 in their country [5]. This delay can also cause infected patients to interact with healthy patients so that the spread of the disease is increasingly widespread. Expensive screening methods with slow results can lead to further spread of the disease and make the situation worse.

The other methods for detecting COVID-19 are analysis of clinical symptoms, epidemiological history, positive results on radiographic images (Computed Tomography (CT) or chest X-rays), and positive pathogen testing [6]. A radiographic image is an image derived from the use of X-rays to form an image of the object under study. Although chest radiography images can aid in the examination of suspected cases of COVID-19, images of various viral pneumonia look similar and sometimes overlap with other lung diseases. Based on the data from WHO, the most common diagnosis in COVID-19 patients is severe pneumonia [7]. In a study conducted in China, 91.1% of 1099

patients were diagnosed with pneumonia by doctors [8]. The resemblance of COVID-19 to other pneumonia viruses makes it difficult for radiologists to distinguish between the two. Thus, this similarity is dangerous because it can lead to incorrect diagnoses in situations where hospitals are overcrowded and health workers have to work around the clock. Misdiagnosis can lead to mishandling which can be mentally and materially detrimental. A chest X-ray is a primary test for detecting pneumonia in a patient, but this test is not as accurate as a CT scan. However, chest X-rays are still useful because they are cheaper, expose the patient to less radiation, and have a wider range than CT scans [9][10]. In addition, X-ray radiation has the potential to cause cell damage, so X-rays can only be done if there are medical indications for the patient. However, in conditions of a lack of tools and experts who can perform rt-PCR swab tests, X-rays can be used to diagnose COVID-19.

To help doctors confirm the patient's condition, an approach that can classify chest radiography images is needed, one of which is using Artificial Intelligence (AI). The application of AI can help doctors in providing diagnoses and reduce the possibility of human error because AI can see features and recognize patterns that are not visible. AI also has the ability to auto featuring. One of the widely used AI systems is Artificial Neural Network (ANN). The advantage of ANN is that it can learn the unknown relationship between input and output data. This allows ANN to study the data according to the amount of data we provide. The quality of the model generated by the ANN method is influenced by the quality of the data. Therefore, the ANN method requires feature extraction on the data so that the existing data can be classified properly. Several feature extraction techniques that can be used are Discrete Wavelet Transform (DWT) and Moment Invariant. DWT has the advantage that it can divide the image into 4 subbands that have average detail, horizontal detail, vertical detail, and diagonal detail. The chest radiograph image used in this study has drawbacks, namely that some images are rotated several degrees to the right or to the left. Therefore, Moment Invariant was chosen because it can recognize the image even though the image undergoes treatments such as rotation, translation, and mirroring.The results of feature extraction will later be used to conclude whether an image is detected by COVID-19 or not.

Previous research on fracture recognition with Haar Wavelet Transform and Backpropagation ANN (BP-ANN) resulted in an accuracy of 93.4% [11]. In addition, the use of Moment Invariant and ANN classifier on weed detection resulted in an accuracy of 92.5% [12]. Another study showed that brain tumor classification with Haar Wavelet Transform and other BP-ANN resulted in an accuracy of 99.2%. [13].

Based on this explanation, the authors propose a study to design a machine learning model to predict COVID-19 through radiographic images using the ANN method with DWT feature extraction and Moment Invariant which is expected to be a model to help medical experts in the health sector

2. LIRATURE REVIEW AND THEORY

Research related to radiographic image recognition has been widely carried out as a tool that helps medical experts in the health sector. Research on the introduction of COVID-19 has been carried out several times. Previous research carried out the classification of COVID-19 using the Deep Neural Network (DNN) and Convolution Neural Network (CNN) methods and obtained an accuracy of 83.4% and 93.2%, respectively [14]. CVDNet, a deep CNN model built to classify COVID-19, pneumonia, and normal using x-ray images that have an accuracy of 96.69% [15].

Another research on radiographic images applies ANN to detect breast cancer. This study obtained an accuracy of 96.3% by extracting the characteristics of contrast, correlation, energy, and homogeneity with the Gray-Level Co-occurrence Matrix (GLCM) method [16].

In another radiographic image study that has six classes, namely the spine, chest, palms of the hands, skull, and head, it was found that the BP-ANN method was the best method with an accuracy of 88.5% [17]. Another method, namely K Nearest Neighbor (KNN) gets an accuracy of 84.3% and the Support Vector Machine (SVM) method gets an accuracy of 82.1%.

In the health sector, moment invariant research was conducted to classify Alzheimer's disease based on the MRI image [18]. This study resulted in an accuracy of 91.4% using the KNN method and 100% for the SVM method. Another study using DWT and ANN was carried out to divide parts of the brain with an accuracy result of 94.8% [19].

Another research in the health sector that applies the haar DWT filter and ANN is carried out to detect fractures with the addition of a Scale-Invariant Feature Transform feature extraction followed by K-means clustering with an accuracy of 93.4% [11]. Research to detect minor chronic cerebral hemorrhage using ANN and DWT feature extraction and Principal Component Analysis resulted in an accuracy of 88.43% Another study that applied moment invariant and ANN was conducted to classify weed, resulting in an accuracy of 92.5% [12].

Based on previous studies, it can be seen that the ANN method with DWT feature extraction and moment invariant can work well for classifying radiographic images. Therefore, a study was conducted that combines

the two feature extraction methods with the hope that the model will work well in recognizing COVID-19 so that it can be useful as a supporting tool in the health sector.

2.1 Theory

1. COVID-19

Corona Virus Disease or COVID-19 is an infectious disease caused by coronavirus. The disease was unknown before the outbreak began in Wuhan, China in December 2019 [1]. The first COVID-19 case in Indonesia was found on 02 March 2020 [20].

Based on the data from WHO, the most common diagnosis in COVID-19 patients is severe pneumonia [7]. Pneumonia is an infection of the part of the lungs responsible for the gas transfer process (alveoli, alveolar ducts, and respiratory tract), called lung parenchyma which is usually caused by different organisms, such as viruses, bacteria, or fungi. Pneumonia cannot be classified as a disease single, but rather a group of different infections with different characteristics [21].

2. Radiographic Image

A radiographic image is an image derived from the use of X-rays to form an image of the object under study. Radiographs are generally used to view opaque objects, such as the inside of a human body. One way to get this radiographic image is with an X-ray. X-ray is an examination procedure using electromagnetic wave radiation to display an image of the inside of the body. Images of solid objects such as bone or iron are shown as white areas, the air in the lungs will appear black, and images of fat or muscle are shown in gray.

3. Discrete Wavelet Transform (DWT)

DWT is a transformation that decomposes a given signal into several sets, where each set is a time series coefficient that describes the time evolution of the signal in the corresponding frequency band [22].

4. Moment Invariant

Moment Invariant is a non-linear function that is invariant to rotation, translation, and scale in the geometric moment of the image. Moment invariant transforms the image function f(x,y) on a discrete system where x is the row and y is the column [23].

5. Artificial Neural Network (ANN)

ANN is an information processing technique inspired by the workings of the human nervous system. The layers that make up the artificial neural network are the input layer, the hidden layer, and the output layer, each of which has neurons.

6. Backpropagation ANN

Backpropagation is an algorithm to minimize errors by adjusting the weights based on the desired output and target. The Backpropagation algorithm for neural networks is generally applied to multilayer perceptrons. Backpropagation involves 3 stages, namely the feed-forward training pattern, error calculation, and weight adjustment.

3. METHODS

3.1 Materials and Tools

The dataset used in this study is a chest radiography image dataset [24] which consist of three classes, namely COVID-19, pneumonia, and normal. The number of images for each class is 1345 images. Images from each class are in image format with a resolution of 1024x1024 pixels.

The tools used in this research process are divided into two parts, namely:

1. Hardware

The hardware used in this research is a computer with the following specifications:

Table 1. Requirement of Hardware

No.	Hardware	Specification
1	Prosesor	AMD A9-9420 Radeon R5, 5 Compute Cores 2C @ 3.00GHz x 3
2	GPU	Radeon R5
3	RAM	4 GB

2. Software

The software used in this study, namely:

Table 2. Requiement of Software

No.	Software	Specification
1	Operating System	Windows 10 64bit
2	Programming Language	Python 3.8.5
3	Microsoft Office	Office 2019
4	Text Editor	JupyterLab, Visual Studio Code

3.2 Research Flowchart

The flow diagram for the system from data collection to reporting is shown in Figure 1.

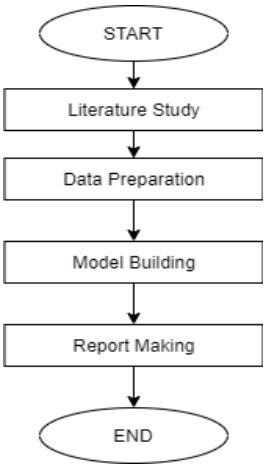

Figure 1. Research flowchart.

3.3 Literature Study

To support the research, it is necessary to conduct a literature study by studying books, research journals, and other sources related to the issues raised. The material studied is related to research related to radiographic images, DWT method, moment invariant, BP-ANN along with the accuracy of each method application. Literature studies are carried out by watching learning videos, searching for journals and e-books on the internet and reading printed books.

3.4 Data Preparation

In this study, machine learning models were made using a dataset of chest radiography images in the form of COVID-19, pneumonia, and normal. The data is a dataset collected by a research team from Qatar University, Qatar, and the University of Dhaka, Bangladesh with their collaborators from Pakistan and Malaysia. There are 15153 images in the dataset for the three classes which will be randomly selected and will be distributed into training data and test data. The image of each image format with a resolution of 1024x1024 pixels [24]. The amount of data that is imbalanced in each class can cause problems related to the performance of machine learning models that are built due to under-represented data and skewed class distribution [25]. This problem can be overcome by various methods, one of which is resampling the dataset. Resampling of this dataset can be done in two ways, namely undersampling and oversampling. In this study, the main concern is to reduce the number of false normals because this error is the most dangerous error compared to false pneumonia and false COVID-19. So, undersampling is done by reducing the size of the abundant class so that the data is balanced.

Figure 2. COVID-19 class dataset.

Figure 3. Pneumonia class dataset.

Figure 4. Normal class dataset.

In the chest radiography images of COVID-19 and pneumonia presented in Figure 2 and 3, both have characteristics of white spots on the lungs with a certain intensity, but the intensity of white spots on the chest radiography images of COVID-19 has a different pattern, which the model will study later. Whereas in the normal chest radiograph in Figure 4, the dominant part of the lung is black which indicates the presence of air in the lungs.

3.5 Model Building

In general, the design of the COVID-19 prediction model has two main processes, namely training and testing, can be seen in Figure 5.

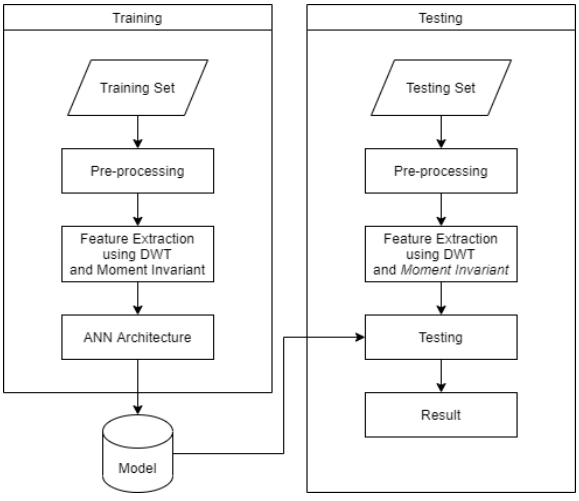

Figure 5. Training and testing process

The two main processes are described as follows:

1. Training Process

The training process includes the following stages:

a. Image dataset measuring 1024x1024 pixels will be converted into grayscale, resizing, and normalized, and then stored as training data.

b. The features of the dataset will be extracted using the DWT method and moment invariant then the distribution of the training data will be used as input data in the classification process using BP-ANN.

c. The classification process is carried out using the BP-ANN method.

d. The resulting model will then be saved after the training process is complete.

2. Testing Process

The testing process includes the following stages:

a. The distribution of datasets that act as test data will not be used in the training process.

b. The saved model will be used as a classifier to classify the test data.

c. The prediction results of the overall test data are used for the values of the model testing methods, namely confusion matrix, precision, and recall.

3.5.1 Pre-processing

The process carried out before the training stage is pre-processing, which consists of converting the image into one dimension (grayscale) then the image size into variations that will be used are tested, namely 64x64, 128x128, and 256x256. Then the image will be normalized by dividing each pixel by 255 to convert it to a normal scale. This is necessary because the variation in the image is quite high. The pre-processing stage is presented in Figure 6.

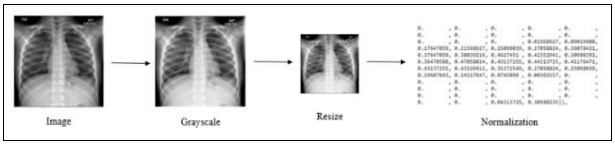

Figure 6. Pre-processing process.

3.5.2 Feature Extraction

The image resulting from the pre-processing stage will then enter the feature extraction stage using the DWT and moment invariant methods. The filter used in the DWT is a first-order Daubechies wavelet (Haar). This step is carried out using the "PyWavelets" library to get the approximation, horizontal, vertical, and diagonal components that will be used as input to calculate the statistical value. The calculated statistical values are the mean, variance, and energy. The extraction process using the DWT method is presented in Figure 7.

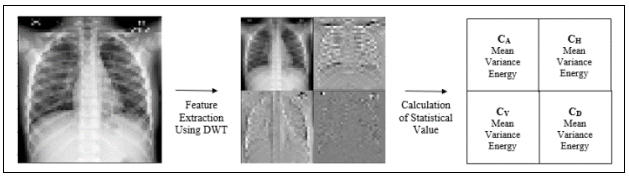

Figure 7. Feature extraction using DWT.

Furthermore, the approximation component (C_A) which is the component that most closely resembles the original image will be extracted using the moment invariant method. The extraction process using the moment invariant method is presented in Figure 8.

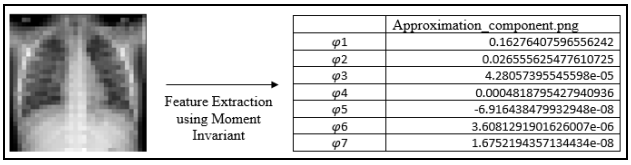

	Approximation_component.png
φ1	0.16276407596556242
φ2	0.026555625477610725
φ3	4.280573955455598e-05
φ4	0.0004818795427940936
φ5	-6.9164384799932948e-08
φ6	3.608129190162600 7e-06
φ7	1.6752194357134434e-08

Figure 8. Feature extraction using moment invariant.

3.5.3 Training

The training parameters in this study consisted of training epochs or iterations of 500 times with a batch of 32, which is the number of images taken for each iteration of the training process. Batch is used to reducing the load of the loaded memory. At the training stage, the cost calculation of the weight used in the model is carried out. The value of this cost becomes the material for evaluating the model to perform optimization by updating the weights on the model. Thus, the model tends to experience an increase in accuracy at each epoch.

4. RESULTS AND DISCUSSION

4.1 Testing

Tests are carried out with the aim of knowing the performance of the model to recognize COVID-19 images. The model's performance is based on:

1. Confusion Matrix

The confusion matrix is a method to evaluate the result of model's performance in training stage. The confusion matrix used in this study is a 2x2 confusion matrix consists of *actual class* dan *predicted* class. True COVID-19 (TCOVID) is a COVID-19 class that is

predicted to be a COVID-19 class. False COVID-19 (FCOVID) is a pneumonia class or normal that is predicted to be a COVID-19 class. True Pneumonia (TPneu) is a pneumonia class that is predicted to be a pneumonia class. False Pneumonia (FPneu) is another class that is predicted to be a class of pneumonia. True Normal (TNormal) is a normal class that is predicted to be a normal class. False Normal (FNormal) is another class that is predicted to be a normal class.

Table 3. Confusion Matrix

		Predicted Class		
		COVID-19	Pneu-monia	Normal
Actual Class	**COVID-19**	TCOVID	FPneu	FNormal
	Pneumonia	FCOVID	TPneu	FNormal
	Normal	FCOVID	FPneu	TNormal

The calculation of model accuracy from the COVID-19 class can be done with Equation (1).

$$accuracy = \frac{(TCOVID)+(TPneu)+(TNormal)}{Total} \quad (1)$$

2. Precision

The precision is the level of accuracy of the model to predict the class that corresponds to the actual class. Precision is useful for determining the impact of false COVID-19 (in the COVID-19 class), where the model detects another class as COVID-19 class, which means the precision is low. The calculation of the precision model for the COVID-19 class can be done by Equation (2).

$$precision = \frac{(TCOVID)}{(TCOVID)+(FCOVID)} \quad (2)$$

3. *Recall*

The recall is the success rate of the model in retrieving information. Recall is useful for determining the impact of false normal and false pneumonia on the actual class of COVID-19, where the model should detect the input as COVID-19 but the model makes an error, which means the recall is of low value. This is dangerous because the model that is built should be able to classify the COVID-19 class well to minimize errors that cause the COVID-19 class to be unpredictable. Recall calculation of the model for the COVID-19 class can be done by Equation (3).

$$recall = \frac{(TCOVID)}{(TCOVID)+(FPneu)+(FNormal)} \quad (3)$$

4.2 Testing Mechanism

There are several steps taken to get the model with the best results. The first stage is to select 1345 images from each class so that the image distribution for each class is evenly distributed. Furthermore, the image will go through the pre-processing and feature extraction stages and will then be divided into 2 parts, namely the training set and the testing set with a distribution of 80% for the training set and 20% for the testing set. The testing phase of the machine learning model was built using several test parameters in the following order:

1. Hidden layer neuron size (64, 96, and 128 *neuron*)
2. Number of *hidden layers* (2 and 3 *hidden layer*)
3. *Learning rate* value (0.001, 0.005, and 0.01)
4. Input image size (64x64, 128x128, and 256x256)

The initial parameters used in the test are a model that has two hidden layers with 64 neurons in each layer, a learning rate of 0.001, and an input image size of 64x64 pixels. The initial parameter value is determined based on the smallest value of each test parameter. To validate and avoid bias in data sharing, the best model will be testing data sharing with k-fold cross-validation using the value of K = 1-10.

4.3 Testing Result

4.3.1 Testing on the number of hidden layer neurons

Variations in the number of hidden layer neurons will produce different performances depending on the image case being handled. In this study, three variations of the number of neurons were used for each hidden layer, namely 64, 96, and 128. The performance of each variation in the number of neurons is presented in Table 4.

Table 4. Test Results On The Number Of Hidden Layer Neurons

Case	HL1	HL2	Accuracy (%)	Testing Loss	Precision (%)	Recall (%)
1	64	64	86	0.41	87	86
2	64	96	86	0.43	86	86
3	64	128	87	0.39	86	86
4	96	64	85	0.41	85	85
5	96	96	85	0.45	86	85
6	96	128	85	0.40	85	85
7	128	64	87	0.39	87	87
8	128	96	86	0.40	87	86
9	128	128	86	0.40	86	86

Based on the test results in Table 4, it was found that the performance of the model with 128 neurons in the first hidden layer and 64 neurons in the second hidden layer was better than the other variations. Thus,

testing for the next parameter uses an architecture with 128 and 64 neurons in the hidden layer, respectively.

4.3.2 Testing the number of hidden layers

The addition of a hidden layer to the architecture is needed to improve accuracy because the data is divided non-linearly. The best number of hidden layers in a neural network architecture does not have a definite determination. The less or more the number of hidden layers will not necessarily increase the accuracy of the model built. Therefore, this study will also use the number of hidden layers as a test parameter. The test parameters are 2 and 3 hidden layers, wherein the third hidden layer there are 3 variations in the number of neurons, namely 64, 96, and 128. The results of model testing on the number of hidden layers can be seen in Table 5.

Table 5. Test Results On The Number Of Hidden Layer

Hidden Layer	Accuracy (%)	Testing Loss	Precision (%)	Recall (%)
2	87	0.39	87	87
3 (64 Neuron)	85	0.45	85	85
3 (96 Neuron)	83	0.46	83	83
3 (128 Neuron)	85	0.50	85	85

Based on the test results in Table 5, the best performance of the model is an architecture with two hidden layers when compared to architecture with three hidden layers. This is because more hidden layers allow the model to learn unnecessary data or noise. So, two hidden layers are good enough to be used in this research. Furthermore, the architecture with two hidden layers is still used for the next test parameters.

4.3.3 Testing the value of learning rate

Learning rate is one of the test parameters that works to calculate the weight correction value during training. Similar to the previous test parameters, the learning rate does not have certain conditions. The lower or higher the learning rate value, the accuracy of a model will not necessarily increase. In this study, three variations of the learning rate were used, namely 0.001, 0.005, and 0.01. The test results on the learning rate value are presented in Table 6.

Table 6. Test Results On The Value Of Learning Rate

Learning Rate	Accuracy (%)	Testing Loss	Precision (%)	Recall (%)
0.001	87	0.39	87	87
0.005	87	0.43	87	87
0.01	85	0.44	85	84

Based on the test results in Table 6, the accuracy, precision, and recall of the learning rate values of 0.001 and 0.005 are the same. However, the testing loss of a learning rate of 0.001 is less than a learning rate of 0.005. It is concluded that the performance of the model with a learning rate of 0.001 is better than that of a learning rate of 0.005 and 0.01. This shows that in the built model, the more frequently the weight is updated, the smarter the model is to study the existing variations. Thus, the previous learning rate value will still be used for the next test parameter.

4.3.4 Testing the size of the input image

The size of the input image in the neural network model is one of the things that affect the performance of the model. This is due to the smaller the size of the image, the less image information, on the other hand, the larger the image size, the greater the computational cost required and too much image information tends to cause overfitting of the model. In this study, three variations of image size will be tested, namely 64x64, 128x128, and 256x256 pixels. The test results can be seen in Table 7.

Table 7. Test Results On The Input Image Size

Input image size	Accuracy (%)	Testing Loss	Precision (%)	Recall (%)
64x64	87	0.39	87	87
128x128	87	0.36	88	88
256x256	84	0.42	85	84

Based on the test results in Table 7, the performance of the 64x64 and 128x128 pixel image input sizes has very little difference. However, the value of the testing loss, precision, and recall of the input image size of 128x128 pixels is better than the image with a size of 64x64 pixels. So, it can be concluded that the best image input size parameter is 128x128 pixels. Based on these results, it can be seen that an image size that is too large can make the model learn unnecessary information and vice versa, an image size that is too small cannot provide sufficient information for the model to learn.

So, it can be concluded that based on the test results on each test parameter, which can be seen in Figure 4.5, the four best parameters are obtained. This parameter is a fully connected neural network architecture that has two hidden layers with 128 neurons in the first hidden layer and 64 neurons in the second hidden layer. Furthermore, the best learning rate obtained is 0.001 with the best input image size is 128x128 pixels.

Thus, the best model has been obtained based on the test parameters contained in the research mechanism. The results of the confusion matrix and the

best performance obtained can be seen in Table 8 and Table 9.

Table 8. The Best Model Testing Confusion Matrix Results

		Predicted Class		
		COVID-19	Pneumonia	Normal
Actual Class	COVID-19	258	16	11
	Pneumonia	11	211	28
	Normal	7	26	239

Table 9. The Best Model Test Performance Results

Accuracy (%)	Precision (%)	Recall (%)
87.73	88	88

Table 9 shows that the best model based on the previous test parameters can perform image classification very well with an accuracy rate of 87.73%, the precision of 88%, and recall 88%.

A high recall value indicates that the model can recognize true COVID-19 well and reduce the number of false normal and false pneumonia. Recall performance is very important in this case because the risk of the actual COVID-19 image being classified as false normal or false pneumonia is less.

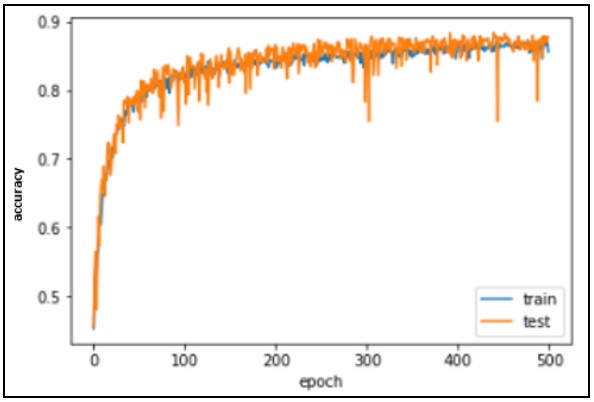

Figure 9. Diagram of the Best Testing and Training Model Accuracy Results

In Figure 9 it can be seen that the model's accuracy performance for training and testing data at 500 epochs was quite good and did not experience overfitting or underfitting. This is because the biggest difference in model accuracy on training data and testing data is not too far, which is 0.02 or 2%, with a training accuracy value of 86%. This difference in accuracy occurs because the model learns more noise or unnecessary data in the training data. Noise in the data in the form of writing on the image, breathing apparatus, and body parts other than the lungs.

4.3.5 Data sharing test

Next, testing the data sharing with k-fold cross-validation on the best model. The previous data sharing technique, namely hold-out validation, has a drawback because the accuracy obtained for one test set can be very different from the accuracy obtained for a different test set. So, a data-sharing test was carried out with k-fold cross validation which can divide the data into some k groups and ensure that each group is used for testing.

The k values or fold values that will be used as test parameters are 2, 3, 4, 5, 6, 7, 8, 9, and 10. In each variation of the k value, 1 fold will be taken which becomes the train data or test data. The results of the data-sharing test include the following:

Table 10. Test Results on Data-Sharing

k	Accuracy (%)	Testing Loss	Precision (%)	Recall (%)
2	84.61	0.413	84.77	84.55
3	85.30	0.385	85.34	85.31
4	86.05	0.380	86.09	85.98
5	85.55	0.390	85.96	85.52
6	85.68	0.387	85.88	85.58
7	84.73	0.398	85.24	84.85
8	85.58	0.386	85.77	85.71
9	85.23	0.394	85.57	85.09
10	86.32	0.370	86.35	86.26

Based on the test results in Table 10, the value of k = 10 obtains the highest accuracy, precision, and recall values with a train:test data sharing ratio of 9:1. This data sharing resulted in an 86.32% accuracy rate, 86.35% precision, and 86.26% recall. The performance of k-fold cross-validation with a value of k = 10 resulted in the best data sharing with low bias. Details of the calculation of k-fold cross-validation with a value of k = 10 can be seen in the table Table 11.

It can be concluded that the model does not experience underfitting or overfitting because the accuracy obtained with various variations of data distribution is relatively the same. In addition, the values of accuracy, precision, and recall that tend to be stable can be caused by the amount of data quantity being exactly the same and the distribution of dataset types being normal, and having the same relative noise for each class.

Table 11. K-Fold Cross Validation Details K=10

Fold	Accuracy (%)	Testing Loss	Precision (%)	Recall (%)

1	87.13	0.372	87	87
2	88.12	0.366	88	88
3	86.39	0.351	86	86
4	85.15	0.444	85	85
5	89.11	0.332	89	89
6	88.09	0.316	88	88
7	83.62	0.422	84	83
8	86.10	0.367	86	86
9	83.87	0.363	84	84
10	85.61	0.370	86	86

The performance of the model built using ANN with a combination of DWT feature extraction and moment invariant is quite good because the accuracy results obtained are close to similar to previous studies. Although the accuracy obtained is lower, the complexity and computation of the model can also be a benchmark for the performance of a model. In previous studies using the CNN method, the parameters in the model were very large so that the complexity and computation of the model were quite heavy. The comparison of CNN architectural performance[26] with the proposed model can be seen in Table 12.

Table 12. CNN Architecture Performance Comparison and The Proposed Model

No.	Architecture Name	Year	Number of Parameters
1	LeNet	1998	60.000
2	VGG	2014	138.000.000
3	Inception-V3	2015	23.600.000
4	Inception-ResNet	2016	55.800.000
5	Xception	2017	22.800.000
6	Convolutional Block Attention Module (ResNeXt101 (32x4d) + CBAM)	2018	48.960.000
7	Proposed Model	2021	11.011

The number of parameters in the proposed model is 11,011. This number is far less even when compared to the famous first CNN model, LeNet. This shows that the complexity and computation of the proposed model are much lighter than previous studies using the CNN method [15]. The fewer number of parameters will result in lighter computations because fewer parameters will be trained, faster training time, faster inference time, and lighter model size so that it can reach more devices with low specifications.

5. CONLUSION AND SUGGESTION

5.1 Conclusion

Based on the research that has been done, there are several things that can be gathered, including the following:

1. The best parameters obtained in this study are 2 hidden layers with 128 and 64 neurons, 0.001 learning rate, and 128x128 pixels input image size.
2. The best model testing obtained through parameter testing resulted in an accuracy of 87.73%, a precision level of 88%, and a recall rate of 88%.
3. Based on the k-fold cross-validation test conducted to test and verify the model's performance using a k value range of 2 to 10, the best accuracy rate was 86.32%, the precision level was 86.35%, and the recall rate was 86.26% with the best k value is 10.

5.2 Suggestion

The suggestions that the authors give if this research will be continued are as follows.

1. Add a minimum of 5000 data per class to the dataset to improve model performance considering ANN has the potential to process large data.
2. Segmenting the radiographic image to separate the lung area and other areas so that noise in the data is reduced.
3. Added calculation of other DWT statistical methods such as skewness and entropy as model input.
4. Embedding the model on the Android platform or web.

REFERENCES

[1] World Health Organization, "Q&A on coronaviruses (COVID-19)." https://www.who.int/emergencies/diseases/novel-coronavirus-2019/question-and-answers-hub/q-a-detail/q-a-coronaviruses (accessed Sep. 22, 2020).

[2] World Health Organization, "Pesan dan Kegiatan Utama Pencegahan dan Pengendalian COVID-19 di Sekolah," 2020. Accessed: Sep. 27, 2020. [Online]. Available: https://www.who.int/docs/default-source/searo/indonesia/covid19/pesan-dan-kegiatan-utama-pencegahan-dan-pengendalian-covid-19-di-sekolah---indonesian--march-2020.pdf?sfvrsn=5cdfea17_2.

[3] A. Susilo et al., "Coronavirus Disease 2019: Tinjauan Literatur Terkini," J. Penyakit Dalam Indones., vol. 7, p. 45, Apr. 2020, doi: 10.7454/jpdi.v7i1.415.

[4] T. Yang, Y.-C. Wang, C.-F. Shen, and C.-M. Cheng, "Point-of-Care RNA-Based Diagnostic Device for COVID-19," Diagnostics, vol. 10, no. 3. 2020, doi: 10.3390/diagnostics10030165.

[5] A. News, "India's poor testing rate may have masked coronavirus cases," 2020. https://www.aljazeera.com/news/2020/3/18/indias-poor-testing-rate-may-have-masked-coronavirus-cases.

[6] M. E. H. Chowdhury et al., "Can AI Help in Screening Viral and COVID-19 Pneumonia?," IEEE Access, vol. 8, pp. 132665–132676, 2020, doi: 10.1109/ACCESS.2020.3010287.

[7] World Health Organization, "Clinical management of severe acute respiratory infection (SARI) when COVID-19 disease is suspected." https://www.who.int/docs/default-source/coronaviruse/clinical-management-of-novel-cov.pdf (accessed Sep. 25, 2020).

[8] W. Guan et al., "Clinical Characteristics of Coronavirus Disease 2019 in China," N. Engl. J. Med., vol. 382, no. 18, pp. 1708–1720, Feb. 2020, doi: 10.1056/NEJMoa2002032.

[9] W. H. Self, D. M. Courtney, C. D. McNaughton, R. G. Wunderink, and J. A. Kline, "High discordance of chest x-ray and computed tomography for detection of pulmonary opacities in ED patients: implications for diagnosing pneumonia.," Am. J. Emerg. Med., vol. 31, no. 2, pp. 401–405, Feb. 2013, doi: 10.1016/j.ajem.2012.08.041.

[10] G. D. Rubin et al., "The Role of Chest Imaging in Patient Management During the COVID-19 Pandemic A Multinational Consensus Statement From the Fleischner Society," no. July, pp. 106–116, 2020, doi: 10.1016/j.chest.2020.04.003.

[11] C. Basha, T. Padmaja, and G. Balaji, "An Effective and Reliable Computer Automated Technique for Bone Fracture Detection," EAI Endorsed Trans. Pervasive Heal. Technol., vol. 5, p. 162402, Jul. 2018, doi: 10.4108/eai.13-7-2018.162402.

[12] A. Bakhshipour and A. Jafari, "Evaluation of support vector machine and artificial neural networks in weed detection using shape features," Comput. Electron. Agric., vol. 145, pp. 153–160, 2018, doi: https://doi.org/10.1016/j.compag.2017.12.032.

[13] N. Rani and S. Vashisth, "Brain Tumor Detection and Classification with Feed Forward Back-Prop Neural Network," Int. J. Comput. Appl., vol. 146, pp. 1–6, Jul. 2016, doi: 10.5120/ijca2016910738.

[14] S. Hassantabar, M. Ahmadi, and A. Sharifi, "Diagnosis and Detection of Infected Tissue of COVID-19 Patients Based on Lung X-Ray Image Using Convolutional Neural Network Approaches," Chaos Solitons & Fractals, p. 110170, Jul. 2020, doi: 10.1016/j.chaos.2020.110170.

[15] C. Ouchicha, O. Ammor, and M. Meknassi, "CVDNet: A novel deep learning architecture for detection of coronavirus (Covid-19) from chest x-ray images," Chaos. Solitons. Fractals, vol. 140, p. 110245, Nov. 2020, doi: 10.1016/j.chaos.2020.110245.

[16] A. Gautam, V. Bhateja, A. Tiwari, and S. C. Satapathy, "An Improved Mammogram Classification Approach Using Back Propagation Neural Network," in Satapathy S., Bhateja V., Raju K., Janakiramaiah B. (eds) Data Engineering and Intelligent Computing. Advances in Intelligent Systems and Computing, vol. 542, Springer, Singapore, 2018, pp. 369–376.

[17] C. Z. Basha, G. Rohini, A. V. Jayasri, and S. Anuradha, "Enhanced And Effective Computerized Classification Of X-ray Images," in 2020 International Conference on Electronics and Sustainable Communication Systems (ICESC), 2020, pp. 86–91, doi: 10.1109/ICESC48915.2020.9155788.

[18] A. Mohammed, F. al Azzo, and M. Milanova, "Classification of Alzheimer Disease based on Normalized Hu Moment Invariants and Multiclassifier," Int. J. Adv. Comput. Sci. Appl., vol. 8, pp. 10–18, Jan. 2017, doi: 10.14569/IJACSA.2017.081102.

[19] C. M. N. Kumar, B. Ramesh, and J. Chandrika, "Design and Implementation of an Efficient Level Set Segmentation and Classification for Brain MR Images," in Dash S., Bhaskar M., Panigrahi B., Das S. (eds) Artificial Intelligence and Evolutionary Computations in Engineering Systems. Advances in Intelligent Systems and Computing, Springer, New Delhi, 2016, pp. 559–568.

[20] World Health Organization, "Situation Report-42," 2020. https://www.who.int/docs/default-source/coronaviruse/situation-reports/20200302-sitrep-42-covid-19.pdf?sfvrsn=63a4f9f2_2 (accessed Sep. 22, 2020).

[21] G. Mackenzie, "The definition and classification of pneumonia.," Pneumonia (Nathan Qld.), vol. 8. p. 14, 2016, doi: 10.1186/s41479-016-0012-z.

[22] M. Hosseinzadeh, "Robust control applications in biomedical engineering: Control of depth of hypnosis," in Control Applications for Biomedical Engineering Systems, A. T. B. T.-C. A. for B. E. S. Azar, Ed. Academic Press, 2020, pp. 89–125.

[23] R. Yulianti, I. G. P. S. Wijaya, and F. Bimantoro, "Pengenalan Pola Tulisan Tangan Suku Kata Aksara Sasak Menggunakan Metode Moment Invariant dan Support Vector Machine," J. Comput. Sci. Informatics Eng., vol. 3, no. 2, pp. 91–98, 2019, doi: 10.29303/jcosine.v3i2.181.

[24] T. Rahman et al., "COVID-19 Chest Radiography Database," 2020. https://www.kaggle.com/tawsifurrahman/covid19-radiography-database (accessed Sep. 25, 2020).

[25] H. He and E. A. Garcia, "Learning from Imbalanced Data," IEEE Trans. Knowl. Data Eng.,

vol. 21, no. 9, pp. 1263–1284, 2009, doi: 10.1109/TKDE.2008.239.

[26] A. Khan, A. Sohail, U. Zahoora, and A. S. Qureshi, “A Survey of the Recent Architectures of Deep Convolutional Neural Networks,” CoRR, vol. abs/1901.0, 2019, [Online]. Available: http://arxiv.org/abs/1901.06032.